NATIONAL ADVISORY COMMITTEE FOR AERONAUTICS

WARTIME REPORT

ORIGINALLY ISSUED

July 1946 as
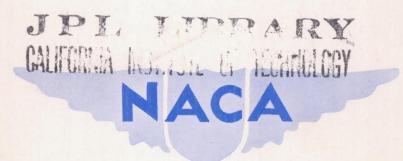Memorandum Report L6F21

FLIGHT INVESTIGATION OF FACTORS AFFECTING

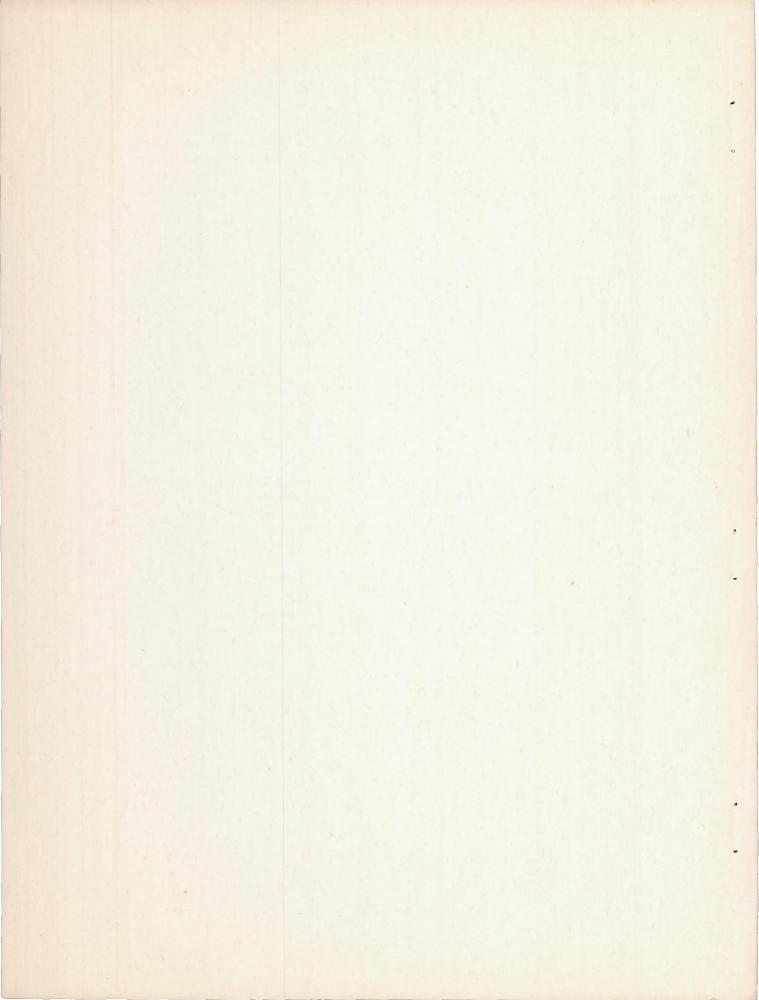THE CARBURETOR RAM AND NACELLE DRAG

OF AN A-26B AIRPLANE

By J. Ford Johnston, Bernard B. Klawans,
and Edward C. B. Danforth, III

Langley Memorial Aeronautical Laboratory
Langley Field, Va.

NACA

WASHINGTON

NACA LANGLEY MEMORIAL AERONAUTICAL LABORATORY

MEMORANDUM REPORT

for the

Air Materiel Command, Army Air Forces

MR NO. L6F21

FLIGHT INVESTIGATION OF FACTORS AFFECTING

THE CARBURETOR RAM AND NACELLE DRAG

OF AN A-26B AIRPLANE

By J. Ford Johnston, Bernard B. Klawans
and Edward C. B. Danforth III

SUMMARY

Flight tests of an A-26B airplane have been conducted to determine the changes in maximum speed, as affected by changes in carburetor ram and aerodynamic refinement of the nacelles, resulting from the addition of sealed spinners and modification of the charge air system, cowling, and nacelle afterbodies. The changes in nacelle drag resulting from these modifications were measured independently by means of a revolving wake survey rake behind the nacelle and boundary layer rakes on the cowling, and provide a quantitative check of the speed measurements as well as a means of analyzing the components of nacelle drag.

The highest carburetor ram, equivalent to an increase of 1600 feet in the high blower critical altitude and 8 miles per hour in top speed over the production configuration, was obtained with the combination of sealed spinners, NACA elbows, and any of the three inlets tested. The optimum configuration for use without spinners was that with the NACA inlets and elbows. This configuration showed an improvement in ram equivalent to 1200 feet in critical altitude and 6 miles per hour in maximum speed over the production configuration.

The sealing of the spinner rear bulkheads caused a further increase in maximum speed of 4 miles per hour through aerodynamic refinement. The substitution of

modified nacelle afterbodies, designed to reduce the pressure drag of the nacelle, produced no speed changes in the spinner-on configuration but appeared to cause an increase of 2 miles per hour in the spinner-off configuration.

Analysis of the nacelle drag with the aid of the revolving wake survey rake indicated that with nominally closed cowl flaps and spinners off the total drag of the two nacelles is over 30 percent of the total airplane drag. The external nacelle drag alone is over 20 percent of the total airplane drag and is composed about 25 percent of cowling drag and 75 percent of afterbody drag. Under the conditions of the tests the afterbody drag was found to vary only with the cooling drag, and the cowling drag to vary only with the cowling inlet-velocity ratio, independently of the use of spinners except as they affected the cooling drag or inlet-velocity ratio. With spinner off only about 50 percent of a given increase in cooling drag appeared as an increase in total nacelle drag because of the accompanying reduction of the afterbody and cowling drags.

Although the nacelle drag is a large portion of the total airplane drag, the external nacelle drag coefficient of about 0.07 based on frontal area is reasonably low. It is indicated that attention should be directed not only toward improving nacelle form, but also toward engine or airplane designs which reduce or eliminate nacelles.

INTRODUCTION

Suggestions for probable increases in the critical altitude and speed of the A-26B airplane through minor design changes to the charge-air induction system were made on the basis of preliminary flight tests of an A-26B airplane at the Langley Laboratory. The Air Materiel Command, Army Air Forces, then requested the NACA to evaluate the effect on performance of these recommendations and other modifications to the cowling and allied nacelle components.

Two objectives were sought; betterment of carburetor ram and aerodynamic refinement of the nacelle. The lower lip of the carburetor-air inlet and the elbow at the carburetor entry were altered in an endeavor to improve

the ram. Drag clean-up was attempted by sealing the spinner rear bulkheads and adding elongated nacelle afterbodies. A special revolving momentum survey rake behind the left engine nacelle was used to facilitate the measurement of the drag changes caused by the modifications.

Concurrently, the Douglas Aircraft Company designed and supplied another carburetor-air inlet for evaluation.

Preliminary test results as necessary for prompt revision of the carburetor-air system were made available to the Air Materiel Command during the course of the investigation. Included herein are the complete results of flight measurements of the effects on speed and critical altitude of the modifications tested, along with a discussion and correlation of nacelle drag measurements by means of momentum surveys.

AIRPLANE

Pertinent details of the production airplane as instrumented for flight test are as follows:

1. Douglas attack bomber, model A-26B, AAF No. 43-22280.

2. Gross weight at take-off including 925 gallons of gasoline, 30,200 pounds.

3. Engines; two Pratt and Whitney R-2800-27, military rating 1600 brake horsepower in high blower at 2700 rpm and 47 inches of mercury manifold pressure; with torque noses for power measurement and jet exhaust stacks siamesed from adjacent cylinders.

4. Propellers; two, three-blade Hamilton Standard, 12 feet, 7 inches diameter; blade drawing No. 6359A-18; gear ratio 0.5:1.

5. Superchargers; two speed, single stage, gear driven; gear ratios; low, 7.6:1; high 9.9:1.

6. Wing span, 70 feet; wing area, 540 square feet.

General views of the production A-26B airplane as flown are shown in figure 1. Additional external details that were added for flight test in all configurations were as follows:

1. Airspeed boom on right wing tip, figure 1(b).

2. Total pressure sources on forwardmost machine gun mounted on fuselage, figure 1(c).

3. Revolving momentum survey rake installed behind the left engine nacelle, figure 1(c).

4. Low-lag free air temperature unit mounted on the under surface of the right wing panel, figure 1(a).

5. Doped fabric seals over ammunition ejection slots, cracks, and holes. No smoothing or fairing of rough or irregular parts was attempted.

The airplane surfaces were free of grease and dust just prior to all test flights.

INSTRUMENTATION

Special instruments installed for the subject tests included synchronized NACA pressure recorders to measure airspeed, altitude, manifold pressures, torquemeter pressures, carburetor metering pressures, and cowling, engine compartment, and carburetor scoop pressures; recording revolution counters for engine rpm; multiple recording manometers, and a 12-unit Miller galvanometer for the static and total pressures and temperatures in the wake of the left engine nacelle.

Free air temperatures were measured with a recording galvanometer connected to an NACA low-lag resistance thermometer bulb on the under surface of the right wing. Flight calibration of the bulb showed that it had an adiabatic rise coefficient of 90 percent. This value was used in reducing the data to ambient conditions.

Uncorrected airspeed impact pressures q_c' were obtained by means of an NACA fixed static head mounted

1-chord length forward of the right wing tip and a shielded total-pressure head located slightly aft and below on the same mount. The position error of this installation was calibrated in flight by comparison with a trailing static head and found to be $-0.01q_c'$ in the high-speed range. This correction was used to determine the correct impact pressure q_c.

Total pressures were measured in the left engine charge-air duct at several stations in order to separate the various sources of pressure drop in the system. Static pressures over the upper and lower inlet lips were obtained by lines of flush orifices as a further check on the alinement of the inlet with the local air flow.

The individual static and total-pressure-measurement locations are given in figure 2. In addition, two total pressure tubes were located at the survey plane just ahead of the carburetor, one close to each side of the duct to check the flow distribution at right angles to the survey shown. Close inspection of figure 3 reveals their positions. Pressures in the boundary layer on the cowling surface were measured at several positions. Figure 4 shows the orifice and tube locations which were the same for all configurations.

Tube locations for measuring pressure recovery H_1 at the front of the left engine are given in table I. The total pressure of the exit engine-cooling air p_2 was measured by taking the numerical average of seven tubes arranged symmetrically about the engine 2 inches ahead of the jet exhaust-stack exits.

It may be noted that duct, cooling-air and boundary-layer pressures were measured only on the left nacelle, as the left and right engine nacelle components were either interchangeable or mirror images.

A feature of the instrumentation was a revolving momentum survey rake behind the left engine nacelle to provide measurements for an analysis of the nacelle drag. The rake revolved in the same direction as the propeller with an angular velocity of $7°$ per second and a tip speed of 4.2 inches per second under which conditions the lag was within the experimental accuracy. The rake contained total-pressure tubes and calibrated static

orifices and iron-constantan thermocouples arranged for continuous recording. The installation is pictured in figure 5, and it may be noted that the rake extends beyond the maximum thickness of the nacelle.

The ship's service indicators were calibrated for instrument error and used to measure cylinder-head temperatures, wing flap, landing gear, and oil shutter positions. Cowl-flap gap indicators with equal and arbitrary scales were placed on the nacelles so that they could be read and the gap set from the cockpit.

TEST SPECIMENS

Outlines of the original, NACA modified, and Douglas modified charge-air ducts are shown in figure 2. It will be noted that the lower lip of the carburetor-air inlet had been cut back about 3 inches for the NACA and 1 inch for the Douglas modification. In addition, the NACA inlet lower lip was given a larger nose radius, and the Douglas inlet upper lip was drooped 3/4 inch. The inner and outer radii of the NACA modified elbow were increased from 1 inch each for the production model to $3\frac{3}{8}$ inches and $7\frac{3}{4}$ inches, respectively. Photographs of the elbows are given in figure 3, and of the inlets in figure 6.

The spinners were sealed by attaching chamois across the rear bulkheads. These seals are illustrated in figure 7. All tests reported with the spinners were made with the seals installed and with the original non-rotating spinner afterbodies.

On some of the later flights, the original nacelle afterbodies were extended 20 inches aft and given chisel tails extending 18 inches above and 13 inches below the horizontal center line to reduce the rate of tail-cone convergence. These new afterbodies are designated the modified nacelle afterbodies and are pictured in figure 5. For ease of construction, the modifications were made in halves and each part was generated from straight lines leading from the afterbody trailing edge to the tail-cone attaching bulkhead. The break in the nacelle lines

over the top at the attaching point was faired out with balsa wood covered with doped fabric.

The carburetor elbow installation in the A-26B is unusual in that the elbow is an integral part of the airframe and must be connected to the inlet and carburetor by flexible joints. The flexible rubber connection between the elbow and the forward section bulged into the duct and consequently reduced the flow area. Cantilever metal plates were installed for four flights in an effort to deflect the bulge down and out of the duct.

TEST PROCEDURE

Tests in all configurations consisted of level-flight runs at and above the high-blower critical altitude. These runs were made with the cowl flaps set nominally closed (full closed as received), oil cooler shutters one-fourth open, and the wing flaps and landing gear full up. Supplementary tests included similar runs made with greater and smaller cowl flap gaps to study the effect of engine cooling drag on the nacelle drag. The engine speed was intended to be 2700 rpm but was limited to about 2660 rpm by a low governor setting.

Three-minute records were taken only after several minutes of a run had elapsed to be sure stabilized conditions had been reached. During these tests, the pilot maintained sensibly constant altitude by reference to a large sensitive altimeter.

One test point per configuration is sufficient to determine the ram and, if accurate, the drag changes for each modification. However, the precision of the individual speed and power measurements leads to possible errors equivalent to ± 2 miles per hour in evaluation of the drag quantity. All tests were run at a series of altitudes, and the results were faired to increase the precision in order to quote comparative changes to 1 mile per hour.

The flight program is outlined in table II. It may be noted that the tests in the table are not chronologically presented but are grouped for comparison purposes. The order of the tests varied from this presentation to expedite the work.

7

RESULTS AND DISCUSSION

Various modifications to the A-26B airplane caused higher level-flight speeds. The following expression is a tool used to separate the causes for the speed increases:

$$V = 52.73 \left(\frac{bhp}{\sigma}\right)^{1/3} \left(\frac{\eta}{SC_D}\right)^{1/3}$$

Measured quantities		Unknown quantities	
V	true speed, mph	η	propulsive efficiency
bhp	engine brake horsepower	C_D	airplane drag coefficient
σ	free-air density ratio		
S	wing area, sq ft		

The parameter $\left(\frac{bhp}{\sigma}\right)^{1/3}$ indicates the contribution of the engine, supercharging, and ram to the speed, and the parameter $\left(\frac{\eta}{SC_D}\right)^{1/3}$ represents the aerodynamic refinement of the airplane-propeller combination. For purposes of the present comparisons the exhaust jet thrust is considered as a contribution to the propulsive efficiency.

Speed and power measurements along with associated data are presented in table I. The speed values given include corrections for a measured gradual increase in drag of the airplane with time and have been further adjusted so that all tests with nominally closed cowl flaps (0.5 gap in table I) have the same engine cooling pressure drop (the corrections are discussed in later sections). Study of these data indicates that 12 miles per hour may be added to the level-flight speed and 1600 feet to the critical altitude of the A-26B airplane through use of the NACA entries and elbows and sealed spinners. Analysis of the parameters, as in figure 8, shows that, of the 12 miles per hour increase, 8 are attributed to an increase in the power parameter and 4 are caused by aerodynamic refinement.

Power Parameter

Factors affecting the power parameter at and above full throttle altitude for the original configuration are compared in figure 9 with those obtained using the most successful set of modifications. It should be noted that power varies approximately as the manifold pressure and, consequently, carburetor pressure for small changes at constant altitude. Therefore, for full throttle operation at a given altitude pressure and temperature

$$\left(\frac{bhp}{\sigma}\right)_1^{1/3} \times \left(\frac{P_{c_2}}{P_{c_1}}\right)^{1/3} = \left(\frac{bhp}{\sigma}\right)_2^{1/3}$$

P_c absolute total pressure at the carburetor collector

Subscripts:

1   original configuration

2   modified configuration

By this analysis, the 7.5 percent increase in the carburetor pressure, in figure 9, explains the total 2.5 percent increase in the power parameter.

Carburetor Ram

The pressure, above stream static, measured at the carburetor total-pressure collector tap is defined for this report as the carburetor ram, as it is a convenient, commonly used single-point source of measurement. This pressure is not necessarily the true total pressure at the carburetor entrance, but is a satisfactory index of changes in ram due to changes in the carburetor-air duct or inlet. Throughout, ram is presented in terms of the airplane impact pressure q_c.

If pressure losses are incurred in the induction system ahead of the carburetor (that is, lowered ram), the maximum altitude at which the rated power of the engines can be obtained is lowered, and performance at all altitudes above the critical altitude is reduced accordingly. The production A-26B airplane had reduced

9

performance as a result of such losses. The modifications designed to improve the carburetor ram of this airplane are discussed in the following paragraphs.

Total and static-pressure data at the various positions in and about the charge-air system on the left nacelle are tabulated in table III. These data were obtained in level flight at and above the full-throttle altitudes. The total pressures at each point of measurement in the duct were arithmetically averaged for all runs in each configuration. From these averaged data, the pressure distributions for pertinent configurations at the carburetor-air inlet and before and after the elbow were obtained and are presented along with the values of carburetor ram in figure 10.

The ram results indicated by figure 10 (parts a-f) are:

Configuration	Figure 10 part no.	Ram in terms of q_c	Ram increase	Change from original configuration due to ram	
				Critical altitude (ft)	Speed (mph)
Original	a	0.41	----	----	-
NACA inlet and elbow	b	.68	0.27	1200	6
NACA inlet and elbow, spinner	c	.76	.35	1600	8
Douglas inlet NACA elbow	d	.50	.09	400	2
Douglas inlet NACA elbow, spinner	e	.74	.33	1500	8
Part c with deflector plate	f	.72	.31	1400	7

Original configuration.- The original carburetor-air
inlet was designed for use with a propeller spinner. When
the spinner was not installed, as was the case with the
production airplane, adverse effects on the recovery at
the entry were noted. The local airflow became more
radial in direction, causing separation off the lower
inlet lip. This separation was so pronounced, as indicated
by the pressure distribution (fig. 10(a)), that the
total-pressure measurements in the lower half of the
entry were not quantitatively useful because of possible
large scale turbulence and reverse flow.

Besides the loss at the entry, part (a) of figure 10
indicates an average loss of $0.11q_c$ in going past the
sharp radii of the original elbow. It is believed, from
inspection of the distributions before and after the
elbow, that the $0.11q_c$ loss is caused primarily by
separation from the inner radius of the turn.

NACA inlet.- The lower lip of the original carburetor-
air inlet was cut-back 3 inches and given a larger radius
(fig. 2) in an attempt to aline the inlet with the local
air flow with the spinner off. This new design, designated
the NACA inlet, resulted in an average improvement of
$0.18q_c$ before the elbow over the recovery with the original
(fig. 10(g)); although the slight drop in total pressure
near the bottom of the inlet (fig. 10(b)) shows that the
lower lip is not perfectly alined. This lower energy
flow appears to have separated at the forward flexible
connection of the elbow causing an average $0.05q_c$ loss
between the inlet and elbow.

Douglas inlet.- The lower lip of the Douglas inlet
was 1 inch farther back and the upper lip was drooped
3/4 inch as compared with the original inlet (fig. 2).
Again, as with the original, the total-pressure measurements
indicate separation at the inlet. It should be noted
that the pressure distribution and level before the elbow
for this configuration were essentially the same as
those obtained with the original entry (fig. 10(h)).
Hence, it is concluded that the Douglas inlet offered no
change in ram recovery over that obtained with the original.

NACA elbow.- The larger radii of the modified elbow
(see fig. 2) reduced the loss of $0.11q_c$ or 0.7 duct q
around the original elbow to $0.03q_c$ or 0.2 duct q.

This reduction was caused mainly by retarding separation from the inner radius of the turn (fig. 10(i)). A loss of 0.2 duct q is about the best obtainable around a 100° turn with the space limitation present, reference 1.

Spinners.- All inlets tested - the original, Douglas, and NACA - had uniform total-pressure distributions and equally good recovery when spinners were used (fig. 10(j)). Data for the original inlet with spinners were obtained from a flight in an intermediate configuration which is not reported in the tables. The uniform distribution is evidence that the spinners satisfactorily alined the local air flow with the inlets.

The maximum-pressure recoveries at the inlets are better with spinners than without. Even the NACA inlet had $0.04q_c$ more maximum-pressure recovery with spinners than without (fig. 10(k)). This improvement is obtained because the spinners cover the inefficient propeller shanks and cause the entry air to pass through the propeller further outboard where the blade sections are more aerodynamically efficient.

Another improvement is the removal of the $0.05q_c$ loss between the NACA inlet and the elbow when spinners are installed. (See fig. 10(k).) The higher energy flow available at the bottom of the inlet with spinners appears to have removed the tendency for flow separation at the flexible joint.

Deflector plates.- The $0.05q_c$ loss between the NACA inlet and elbow, spinner off, is believed to have been caused by separation off the flexible joint ahead of the elbow which might not have occurred in a smooth duct. Accordingly, bent sheets of dural were installed under the bottom clamps at the elbow end of the joint in an attempt to deflect the rubber connection down and out of the carburetor duct.

Tests with and without the deflector plates, spinner on, are compared in figure 10(m) and show an additional loss in ram of $0.04q_c$ caused by the deflector plates. Inspection of the flexible joint after the tests revealed that the rear cowl mounting ring prevented the bulge from deflecting out of the duct. Apparently, the deflector plates reduced the width of the bulge, forcing the bulge to extend further into the duct and cause the additional loss.

Significance of results.- If ram is the criterion, the optimum configuration is that with sealed spinners, NACA elbows, and any of the inlets. These configurations showed a carburetor ram of about $0.75q_c$, an increase of $0.34q_c$ (equivalent to 1600 ft in critical altitude and 8 miles per hour top speed) over that obtained with the original configuration.

An alternate choice available if spinners are undesirable from a maintenance standpoint is the configuration with NACA inlets and elbows. With this configuration a carburetor ram of $0.68q_c$ was obtained, only $0.08q_c$ or 400 feet in critical altitude and 2 miles per hour below the optimum.

The average pressure after the elbow (fig. 10(c)) illustrates that the actual pressure recovery at the carburetor entrance with NACA elbows and sealed spinners was $0.95q_c$, indicating a duct loss of about $0.05q_c$. The only additional improvement available in this case would be to improve the propeller shanks aerodynamically to increase the energy level at the inlet. This actual recovery also indicates that the pressure in the carburetor collector was in this case about $0.20q_c$ below the true total pressure.

Aerodynamic Refinement

The aerodynamic-refinement parameters for three flights, one each at the beginning, middle, and end of the program are presented in figure 11(a). The flight configurations were the same except for the design of the lower carburetor-air inlet lip that should cause negligible changes in drag. Inasmuch as a gradual decrease in the aerodynamic refinement is noted with time, it is concluded that the airplane aged. This aging, brought about principally by flight time and landings, was the result of numerous wrinkles that developed in the fuselage skin along with the spreading of joints and general deterioration (that is, roughening) of the external surfaces. All values quoted for speed and aerodynamic refinement, except those of figure 11, are corrected by the deviations in aerodynamic refinement shown in figure 11(b), to have comparable airplane finishes to that of the middle flight.

Sealed spinners.- It was found in preliminary tests that the spinners, as originally used, caused no change in the aerodynamic refinement. However, when the spinner rear bulkheads were sealed as shown in figure 7, a 4 mile-per-hour increase caused by aerodynamic refinement was measured over that obtained with the spinners off, figure 12(a).

Modified nacelle afterbodies.- Although the modified nacelle afterbodies produce no aerodynamic refinement when sealed spinners are installed, figure 12(b), the afterbodies appear to cause an increase of 2 miles per hour with the production configuration (fig. 12(c)).

Effect of engine cooling drag.- Tests were made with three different cowl-flap positions, spinners off, to determine the variation of aerodynamic refinement with cooling-air pressure drop $H_1 - p_2$. Figure 13 shows the results of these tests. Increments of aerodynamic refinement $\left(\dfrac{\eta}{SC_D}\right)^{1/3}$ measured from the base value obtained at a cooling-air pressure drop of $0.39q_c$ have been plotted against $\dfrac{H_1 - p_2}{q_c}$.

The changes in cooling drag calculated from the cooling pressure measurements have been converted to increments of aerodynamic refinement and are included in figure 13. It is seen that the predicted changes in aerodynamic refinement are always greater than those measured. This difference is apparently caused by compensating variations in the external nacelle drag, as will be shown in a later section.

As previously noted, the speed and aerodynamic refinement values obtained with nominally closed cowl flaps have been corrected to a cooling pressure drop of $0.39q_c$. This correction, from figure 13, did not affect the faired results by more than 0.5 mile per hour.

Nacelle Drag
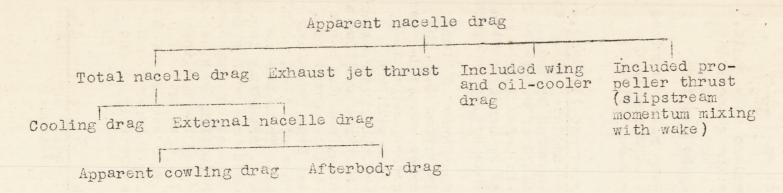
In the preceding section, the changes in drag and propulsive efficiency resulting from the modifications to

14

the nacelle were shown by their effect on $\left(\dfrac{\eta}{SC_D}\right)^{1/3}$,
the aerodynamic refinement of the airplane as a whole.
In order to show more clearly whether the changes in
$\left(\dfrac{\eta}{SC_D}\right)^{1/3}$ were directly the result of the nacelle
modifications, the revolving wake survey rake described
under Instrumentation was installed behind the left
nacelle along with the boundary-layer rakes (fig. 4)
on the cowling.

Effect of modifications on apparent nacelle drag.-
The apparent nacelle drag was obtained by integrating the
positive drag region within the area covered by the
revolving wake survey rake, by the method of reference 2.
This apparent nacelle drag is useful in determining
changes in drag resulting from changes in configuration
provided all tests are run at comparable speeds and powers.

The values of apparent nacelle drag area f for
several configurations are compared in figure 14. The
effect of the addition of sealed spinners was to decrease
f by 0.20 square feet (fig. 14(a)) corresponding to
2 miles per hour per nacelle which agrees with the
2 miles per hour per nacelle found from the speed measure-
ments. Speed measurements indicated that the modified after-
bodies caused no speed change spinner on, but did cause
an increase of 1 mile per hour per nacelle spinner off.
No corresponding improvement in nacelle drag resulting
from the modified afterbody with spinner off (fig. 14(b))
could be detected with the survey rake. There were no
rake measurements made with the original afterbody installed,
spinner on. Increasing the cowling exit area with spinner
off (fig. 14(c)) caused an increase in nacelle drag area of
0.48 square feet corresponding to a reduction in speed of
5 miles per hour per nacelle. Decreasing the cowling
exit area caused a reduction in nacelle drag area of
0.20 square feet corresponding to an increase in speed
of 2 miles per hour. The corresponding changes found
from the speed measurements were, respectively, 6 and
2 miles per hour per nacelle.

Analysis of the components of the apparent nacelle
drag.- The breakdown of the apparent nacelle drag into
its components is shown in the following table:

15

Apparent nacelle drag

Total nacelle drag   Exhaust jet thrust   Included wing   Included pro-
                                              and oil-cooler   peller thrust
                                              drag   (slipstream
                                                                momentum mixing
Cooling drag   External nacelle drag   with wake)

Apparent cowling drag   Afterbody drag

In order to calculate the total nacelle drag, the magnitude of the other three components of the apparent nacelle drag must first be estimated. In the course of the tests, the direct measurement of the exhaust jet thrust was attempted with but little success in the time available. Consequently, the exhaust jet thrust, in the high-speed condition covered by these tests, has been estimated according to the method of reference 3, and found to be equivalent to a negative drag area of about 1.2 square feet. From an examination of the wake drag distributions, the included wing and oil-cooler drag areas appeared to be about 0.3 square foot. Because of the difficulty associated with obtaining this estimate, the error may be as large as ±0.1 square foot.

The calculated drag areas for the exhaust jet thrust and included wing and oil-cooler drag have been subtracted from the faired data of figure 14 to obtain the total nacelle drag, and points for each cowl flap position tested have been plotted in figure 15(a) against the engine cooling drag area calculated from the cooling pressure measurements. The error introduced by the momentum mixing of the propeller slipstream with the nacelle wake is assumed to be small.

During flight 5, not reported in the tables, one run was made with spinner on in a glide at the level-flight test speed with the left propeller feathered and with nominally closed cowl flaps. The survey-rake measurements were thus free from the effects of the propeller and exhaust thrust. The value of total nacelle drag area, 1.9 square feet as corrected for included wing and oil cooler drag, that was obtained on this run may be slightly high since it is possible that the wake of the slowly revolving propeller shanks was not faired completely out of the records. The power-off point, plotted on figure 15(a) at a cooling drag area of 0.72 square foot, shows close agreement with the power-on, spinner-on total nacelle drag. This indicates either that the assumptions with regard to exhaust jet thrust and the effect of the propeller slipstream are correct, or that errors in these assumptions are compensating. Examination of the spacing of the drag contours power off and power on indicated that the mixing of the slipstream extended only a small distance into the nacelle wake and therefore had only a small effect on the total nacelle drag.

The variation of total nacelle drag with cooling drag in the propeller-off configuration as measured in the wind-tunnel tests of reference 4 is included on figure 15(a) for comparison. The cooling drag has been subtracted from the total nacelle drag to obtain the external nacelle drag which, also, is plotted in figure 15(a).

The apparent cowling drag as calculated from the average momentum deficiency at the cowling boundary-layer rakes has been subtracted from the external nacelle drag to obtain the afterbody drag. Both the afterbody drag area and the apparent cowling drag area are plotted against the cooling drag area in figure 15(b). The afterbody drag is noticeably larger than the apparent cowling drag. With spinner off and normal cowl-flap setting, the external nacelle drag is composed about 75 percent of afterbody drag and 25 percent of apparent cowling drag.

The drag of the afterbody is seen to decrease by about one-third the increase in cooling drag and to be independent of the spinner except insofar as the spinner affected the cooling drag. The change in afterbody drag

17

arises principally from a change in the skin-friction drag. As the cooling drag is increased, lower velocity air will flow from the cowling exit with a consequent decrease in the skin-friction drag of the afterbody. The afterbody drag would be decreased by the amount of the reduction in skin friction provided the pressure drag of the afterbody did not change appreciably. As the static-pressure recovery at the rear of the afterbody was sensibly constant for all configurations, there was apparently no significant change in the pressure drag.

The shape of the external nacelle drag variation (fig. 15(a)) as determined from the spinner-on, power-off wind-tunnel tests indicates that, as the cooling drag was increased, the reduction in afterbody skin-friction drag was accompanied by an increase in pressure drag. At cooling drag areas greater than about 1.6 square feet the increase in pressure drag became predominant causing an over-all increase in afterbody drag. No such increase in pressure drag occurred in flight within the range of the tests. In the flight tests, separation of the flow over the afterbody was apparently delayed by the action of the high velocity exhaust gases and the propeller slipstream. The external nacelle drag would begin to increase at some cooling drag area higher than that tested.

It is not expected that the cowling drags spinner off and spinner on would be correlated on the basis of cooling drag, as the momentum defect of the exit cooling air can affect only that portion of the nacelle behind the cowl flaps. For a given configuration, however, a change in cooling drag involves a change in inlet-velocity ratio, and thereby may affect the cowling drag. Figure 15(b) shows that separate curves are obtained for the apparent cowling drag of the two configurations when plotted against cooling drag. The apparent cowling drag area has been replotted in figure 15(c) against the cowling inlet-velocity ratio. All points, both spinner on and spinner off, appear to fall on a single curve indicating that under the test conditions the apparent cowling drag varies only with inlet-velocity ratio. The addition of the spinner decreased the apparent cowling drag but only insofar as the inlet-velocity ratio was increased. Parallel results are indicated in reference 5 for the effect of a spinner on the velocity distribution

over the cowling. In reference 5 it is shown that for this type of cowling the critical inlet-velocity ratio, below which pressure peaks form on the nose of the cowling, is about 0.33. In figure 15(c) it is seen that below an inlet-velocity ratio of about 0.30 the apparent cowling drag begins to rise. This rise in drag is associated with the development of pronounced pressure peaks leading to local separation over the lip of the cowling. Above an inlet-velocity ratio of 0.30, in which range the cowling pressure distribution is smooth, the drag is that to be expected from skin friction alone, and further reductions in apparent cowling drag are negligible. Slightly different results might have been obtained if the spinner-on case could have been extended below inlet-velocity ratios of 0.30 by restricting the air flow. The consequent high adverse pressure gradient along the spinner in this impractical condition would cause separation of the flow ahead of the inlet resulting in unsteady flow not only into the inlet but also over the cowling. It has been shown in reference 6 that under similar conditions the flow over a scoop with a related boundary layer similar to that on a spinner fluctuated from smooth flow with low drag to flow with high pressure peaks and high drag.

In figure 15(a) it is seen that the slope of the curve of total nacelle drag versus cooling drag is lower with spinner off than with spinner on. Since the variation of afterbody drag is the same spinner-on and spinner-off, the difference in slope is caused only by the variation of apparent cowling drag with inlet-velocity ratio. With spinner off the cowling is operating on the steep portion of the curve in figure 15(c) whereas with spinner on it is operating on the flat portion of the curve. This accounts for the more rapid com-pensating variation of external nacelle drag with cooling drag, spinner off. With spinner off, about one-half, and with spinner on about two-thirds of a given change in cooling drag appeared as a change in total nacelle drag.

Distribution of drag in the nacelle wake.- Sample plots of the distribution of point drag coefficient c_d' in the nacelle wake are presented in figure 16. The wake has, in general, a characteristic hour-glass shape indicating low drag on the nacelle sides just below the lower wing-nacelle junctures, and a consequent vertical displacement of the regions of high drag on the upper and

lower surfaces of the nacelle. The wing wake may be seen
projecting from either side of the nacelle wake. The
higher drag of the wing on the outboard side of the
nacelle is probably due to the additional drag of the oil
cooler located at that station. The general spreading
of the wake that occurs upon removal of the spinner is
evident from a comparison of parts (b) and (d) of
figure 16 for the normal cowl-flap position. The increase
in drag with cowling exit area may be seen by comparing
parts (a), (b), and (c) for the spinner-off condition
and parts (d) and (e) for the spinner-on condition.

Significance of nacelle drag measurements.- The
comparisons of the nacelle wake measurements with the
measured speed changes have shown good agreement.
Although the data evaluation is laborious, the results
obtained indicate that wake surveys in three-dimensional
flow offer an effective means for analysis of the drag
or thrust of airplane components such as nacelles under
actual flight conditions.

The results of the flight tests of this report and
the wind-tunnel tests of reference 4 indicate that for
the A-26B airplane the spinner-on external nacelle drag
coefficient, based on frontal area, is about 0.07.
Although this coefficient is reasonably low, the external
drag of the two nacelles is about 20 percent of the total
airplane drag. The total drag of the two nacelles
amounts to about 30 percent of the total airplane drag
in the high-speed condition with normal cowl-flap setting.
These percentages are slightly higher with spinner off.

As the aerodynamic cleanness of airplanes continues
to be improved, the drag of nacelles will become an even
larger portion of the total drag. This proportion
indicates a need not only for continuing improvement of
nacelle form, but also for a thorough reevaluation of the
comparative advantages of engines or airplane designs
which reduce or eliminate nacelles.

CONCLUSIONS

1. Flight tests of modifications to the charge-air
induction system of an A-26B airplane indicate that:

(a) The optimum configuration includes sealed spinners, NACA elbows, and any of the three inlets tested. The total pressure at the face of the carburetor was 95 percent of the airplane impact pressure leading to an improvement over the original of 1600 feet in high blower critical altitude and 8 miles per hour in the top speed, because of increased ram.

(b) The optimum configuration for use without spinners is that with the NACA entries and elbows. An improvement in ram over the original is realized with this configuration and is equivalent to 1200 feet in critical altitude and 6 miles per hour top speed.

2. Analysis of the speed and power measurements indicates that:

(a) Seals over the spinner rear bulkheads caused an improvement in speed of 4 miles per hour through aerodynamic refinement.

(b) The modified nacelle afterbodies produced no speed changes in the spinner-on configuration but appeared to cause an increase of 2 miles per hour in the spinner-off configuration.

3. Analysis of the nacelle drag in the high-speed condition by means of wake surveys indicates that:

(a) Changes in nacelle wake drag were generally in close agreement with the measured speed changes.

(b) With nominally closed cowl flaps and spinners off, the total drag of the two nacelles is over 30 percent of the total airplane drag. The external drag alone is over 20 percent of the total airplane drag.

(c) With nominally closed cowl flaps and spinner off, about 25 percent of the external nacelle drag arises from the apparent cowling drag and 75 percent from the afterbody drag.

(d) Under the conditions of the tests the afterbody drag was found to vary only with the cooling drag, and the apparent cowling drag to vary only
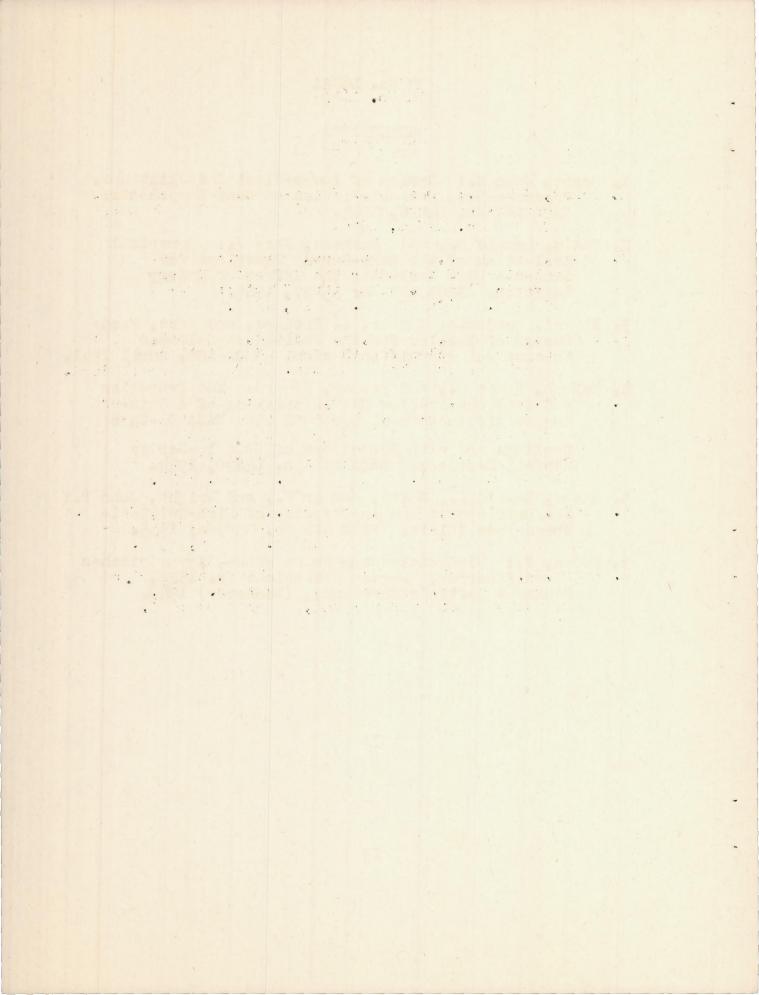
with the cowling inlet-velocity ratio, independently
of the use of spinners except as they affected the
cooling drag or inlet-velocity ratio.

(e) With spinner off, only about 50 percent of
a given increase in cooling drag appeared as an
increase in total nacelle drag because of the
accompanying reduction of the cowling and afterbody
drags.

Langley Memorial Aeronautical Laboratory
    National Advisory Committee for Aeronautics
        Langley Field, Va.

REFERENCES

1. Henry, John R.: Design of Power-Plant Installations.
   Pressure-Loss Characteristics of Duct Components.
   NACA ARR No. L4F26, 1944.

2. Baals, Donald D., and Mourhess, Mary J.: Numerical
   Evaluation of the Wake-Survey Equations for
   Subsonic Flow Including the Effect of Energy
   Addition. NACA ARR No. L5H27, 1945.

3. Pinkel, Benjamin, Turner, L. Richard, and Voss, Fred:
   Design of Nozzles for the Individual Cylinder
   Exhaust Jet Propulsion System. NACA ACR, April 1941.

4. McHugh, James G., and Pepper, Edward: The Propeller
   and Cooling-Air-Flow Characteristics of a Twin-
   Engine Airplane Model Equipped with NACA D_S-Type

   Cowlings and with Propellers of NACA 16-Series
   Airfoil Sections. NACA ACR No. L4I20, 1944.

5. Baals, Donald D., Smith, Norman F., and Wright, John B.:
   The Development and Application of High-Critical-
   Speed Nose Inlets. NACA ACR No. L5F30a, 1945.

6. Ruden, P.: Windkanalmessungen an ebnen, symmetrischen
   Fangdiffusoren. Forschungsbericht Nr. 1325,
   Deutsche Luftfahrtforschung, (Hannover) 1940.

TABLE I

Airplane, ambient air, power, and engine cooling air data

Configuration of tests	NACA inlet & elb					Sp, NACA inlet & elb					Original							Sp, def pl, NACA inlet & elb, aft bd						def pl, NACA inlet & elb, aft bd						NACA inlet & elb					NACA inlet & elb					
Airplane conditions																																									
Flight	1					3					6					7		16					17					18						19					22				24					
Run	1 2 3 4 5					1 2 3 4 5					1 2 3 4 5					1 2		1 2 3 4 5					1 2 3 4 5					1 2 3 4 5 6						1 2 3 4 5					1 2 3 4				1 2 3 4 5 6					
V, mph	348 348 351 350 352					353 355 355 356 356					340 342 344 346 348 338 342							350 350 354 356 357 349 354 358 343					349 350 352 353 353 343 348 348 351 351 351								345 345 348 351				348 348 348 350 352 350					
Qc, in.H2O	354 372 388 402 412					363 376 390 408 414					336 353 387 387 403 326 343							328 339 357 371 382 338 372 404 368					333 347 362 376 388 304 331 332 364 378 388								316 328 347 306				320 331 341 300 374 370					
Q0,in.H2O	341 354 367 384 389					500 498 498 498 499					318 334 347 366 381							315 328 342 355 367 345 363 364 344 355 356 5										299 310 329 347				303 314 323 341 354 351					
M	493 496 496 494 495										577 579 578 581 581 575 578							581 579 582 581 582 588 590 590 570					580 580 580 579 577 583 581 582 580 578 570								488 488 471 473				471 470 467 470 470 468					
Ambient air conditions																																									
hp ft/1000	18.9 18.0 18.9 15.9 15.4					19.0 18.0 17.0 15.9 15.8					18.5 17.5 16.4 15.4 14.4 19.0 18.0							18.5 18.5 17.5 16.5 15.3 18.4 17.4 15.4 15.4					18.0 18.0 16.9 18.0 14.9 14.9 19.2 18.2 16.8 15.7 14.9								18.0 18.0 17.0 18.0				18.0 18.0 17.0 18.0 15.1 15.1					
Po, in. Hg	14.38 14.97 13.61 16.29 16.83					14.38 14.94 15.55 16.25 16.48					14.64 15.27 15.93 16.60 17.28 14.36 14.93							14.03 14.63 15.24 15.90 16.70 14.07 15.29 16.60 16.58					14.38 14.94 15.60 16.24 16.92 16.92 14.20 14.19 15.70 16.38 16.92								14.33 14.92 15.57 16.23				14.34 14.92 15.55 16.22 16.83 16.83					
hd ft/1000	18.6 17.7 16.8 15.5 15.0					19.2 18.3 17.3 16.2 15.9					18.7 17.6 16.7 15.6 14.7 19.3 18.5							20.6 19.7 18.7 17.8 16.5 19.7 17.6 15.7 15.8					20.0 19.0 18.0 17.1 16.0 20.0 20.0 17.6 16.6 15.8								20.6 19.5 18.5 17.4				20.8 19.7 18.7 17.6 16.7 16.7					
To, °F abs	446 451 458 458 458					454 459 461 466 468					455 458 464 466 470 458 461							466 471 474 480 484 452 459 468 469					468 470 474 478 482 482 462 462 471 475 478								475 477 480 482				478 481 485 486 490 490					
ηa, ft abs	.538 .515 .503 .819 .628					.547 .503 .584 .604 .611					.557 .577 .585 .617 .630 .548 .561							.521 .538 .558 .574 .598 .539 .577 .814 .612					.533 .550 .569 .588 .608 .608 .532 .532 .577 .597 .613								.522 .541 .561 .582				.519 .538 .558 .577 .594 .595					
Power measurements																																									
bhp L	1302 1376 1444 1486 1528					1335 1369 1430 1490 151					1242 1301 1346 1403 1480 1206 1283							1270 1312 1359 1409 1474 1288 1391 1500 1484					1286 1335 1390 1433 1181 1482 1281 1257 1377 1426 1489								1229 1269 1320 1377				1229 1263 1291 1352 1374 1415					
rpm L	2880 2680 2890 2880 2880					2870 2670 2680 2670 2680 2670 2670					2880 2880 2880 2670 2680 2670 2670							2880 2680 2680 2680 2680 2880 2680 2680 2660					2670 2670 2670 2670 2680 2670 2670 2680 2660 2670 2670								2880 2860 2880 2880				2660 2650 2640 2660 2640 2650					
CMP L	50.9 53.9 58.9 62.7 63.6					47.8 51.2 55.4 58.9 60.5					42.6 50.8 54.6 520 63.9 44.2 47.8							43.2 40.0 48.1 52.1 52.4 40.5 54.1 61.3 60.8					44.4 47.5 50.1 54.6 58.4 44.4 44.4 51.9 55.1 58.4								41.0 44.3 48.2 51.6				30.0 32.1 41.7 46.6 42.7 51.4					
Engine cooling air measurements, in pressure coefficient form, (h-p0)/qc																																									
s cyl. 5	.90 .91 .91 .92 .92					.87 .87 .87 .88 .86					.88 .88 .88 .86 .86 .85 .84 .87 .86							.91 .91 .91 .91 .91 .90 .90 .90 .90 .90 .90										.89 .89 .89 .90				.88 .88 .88 .88 .89 .90					
s cyl. 6	.94 .93 .93 .93 .93					.88 .88 .88 .88 .87					.93 .94 .93 .92 .93 .93 .93							.87 .86 .87 .87 .87 .87 .88 .87 .90					.91 .91 .91 .91 .91 .90 .90 .90 .90 .90 .90								.91 .92 .92 .92				.91 .91 .91 .90 .90 .90					
H, .5	.90 .89 .89 .89 .89					.83 .84 .83 .83 .81					.89 .89 .88 .89 .89 .89 .90							.83 .82 .82 .83 .82 .82 .84 .82 .82					.88 .88 .87 .87 .87 .87 .88 .88 .87 .87 .87								.89 .88 .88 .88				.88 .88 .88 .88 .88 .88					
ctg	0.5 0.5 0.5 0.5 0.5					0.5 0.5 0.5 0.5 0.5					0.5 0.5 0.5 0.5 0.5 3.0 3.0							0.5 0.5 0.5 0.5 0.5 0.5 0.5 0.5 0.5					0.5 0.5 0.5 0.5 0.5 0.5 0.5 0.5 0.5 0.5 0.5								0.5 0.5 0.5 0.5				-0.5 -0.5 -0.5 -0.5 -0.5 0.5					

Abbreviation definitions

Configuration		Airplane conditions		Ambient air conditions		Power measurements	
inlet	carburetor-air inlets	V	true airspeed, corrected	hp	pressure altitude	L	left engine
elb	carburetor duct elbows	Qc	airplane impact pressure	po	altitude pressure	R	right engine
Sp	spinners	Q0	free-stream dynamic pressure	hd	density altitude	bhp	brake horsepower
def pl	deflector plates	M	free-stream mach number	To	free-air temperature	rpm	engine revolutions per minute
aft bd	modified nacelle afterbodies			ηa	free-air density ratio	Pm	engine manifold pressure, in Hg
						Ram	pressure at carburetor collector tap above stream static/qc
						CMP	compensated metering pressure, in H2O
						UMP	uncompensated metering pressure, in H2O
						Tc	carburetor air, taken as free-stream stop temperature

Engine cooling air measurements

- s — side of head of front cylinder located in the cooling fins facing toward
- cyl. — cylinder
- t — top of head of front cylinder located in the center cooling fins facing foward
- b — side of barrel of front cylinder located in the middle cooling fins facing foward
- H₁ — average front engine cooling air pressure taken as the numerical average of the six measured
- r — rear of head of rear cylinder (static)
- p2 — average rear pressure taken as numerical average of seven total head tubes located in cowl flaps
- H₁-p2 — cooling air pressure drop across engine
- h — measured total pressure
- ctg — cowl flap gap, in arbitrary units

NATIONAL ADVISORY
COMMITTEE FOR AERONAUTICS

TABLE II

FLIGHT PROGRAM

Flight	Carburetor air inlet	Spinners	Elbows	Afterbodies	Deflector plates	Remarks
6, 7	Original	Off	Original	Original	None	The base configuration - all changes referred to these flights.
1	NACA modified	Off	NACA modified	Original	None	Original entry and elbows replaced by the NACA modifications.
22	NACA modified	Off	NACA modified	Original	None	Repeat of flight 1 - to check a suspected gradual increase in over-all drag with time.
24	NACA modified	Off	NACA modified	Original	None	Repeat of flights 1 and 22 with a smaller cowl-flap gap.
18, 19	NACA modified	Off	NACA modified	Modified	Installed	Same as flights 1 and 22 except for elongated afterbodies and the deflector plates.
3	NACA modified	On	NACA modified	Original	None	Same as flights 1 and 22 with the sealed spinners installed.
16, 17	NACA modified	On	NACA modified	Modified	Installed	Repeat of flight 3 with the elongated afterbodies and the deflector plates.
[1]14, 15	Douglas modified	Off	NACA modified	Modified	None	Ram check of the Douglas entry without spinner.
[1]13	Douglas modified	On	NACA modified	Modified	None	Ram check of the Douglas entry with spinner.

[1]Only one Douglas inlet was available for these tests. The original inlet with NACA modified elbow, sealed spinner and elongated nacelle afterbody was used on the right engine nacelle. For all other tests, both nacelle configurations were the same.
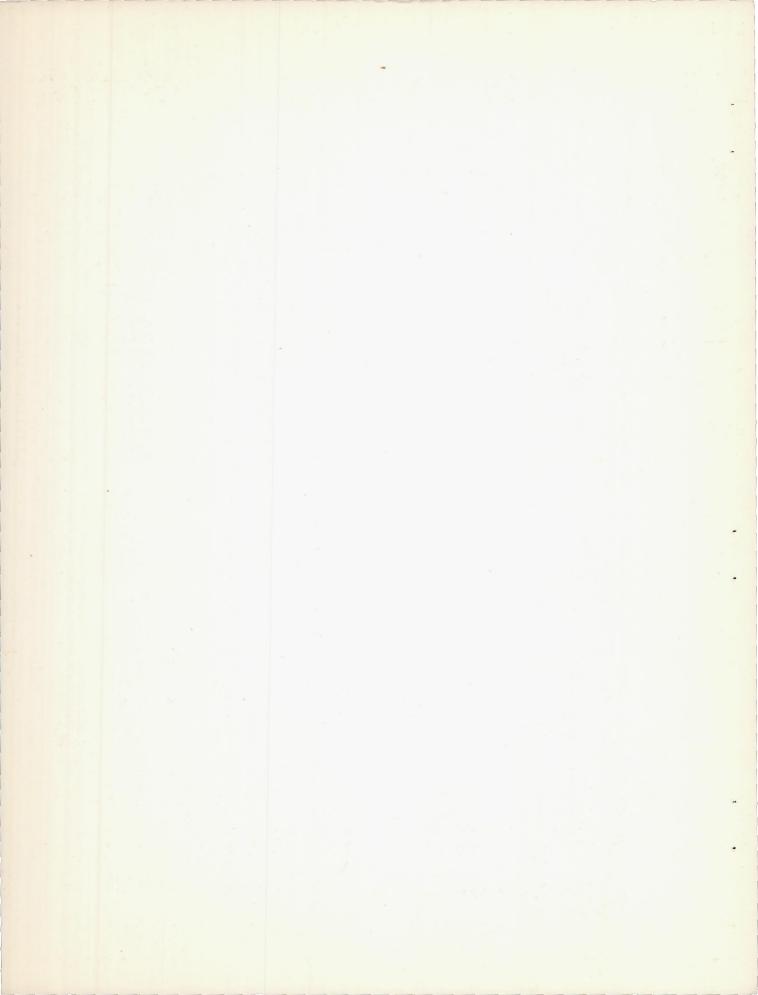
NATIONAL ADVISORY
COMMITTEE FOR AERONAUTICS

TABLE III

Carburetor-air inlet and duct airflow data

Configuration of tests / Airplane conditions

		NACA inlet & elb					Sp, NACA inlet & elb					Original					Sp, Dg inlet, NACA elb					Douglas inlet, NACA elb						Sp, def pl, NACA inlet & elb				
Flight		1					3					6					13					14		15				16				
Run		1	2	3	4	5	1	2	3	4	5	1	2	3	4	5	1	2	3	4	5	1	2	1	2	3	4	1	2	3	4	5
Q_c, in H_2O		35.4	37.2	38.8	40.2	41.2	36.3	37.6	39.0	40.8	41.4	33.6	35.3	36.7	38.7	40.3	34.2	35.4	36.7	38.7	40.1	32.8	33.9	35.7	37.1	39.2	38.3	31.0	32.1	33.8	35.1	37.1
Q_o, in H_2O		33.4	35.0	36.5	37.8	38.8	34.1	35.4	36.7	38.4	38.9	31.8	33.4	34.7	36.6	38.1	32.3	33.4	34.6	36.5	37.7	31.0	33.3	35.1	36.0	37.9	36.1					
P_o, in Hg		14.38	14.97	15.61	16.29	16.63	14.36	14.94	15.55	16.25	16.46	14.64	15.27	15.93	16.60	17.28	14.07	14.64	15.27	15.91	16.48	14.06	14.95	15.61	16.26	17.27	16.25	14.03	14.03	15.24	15.90	16.70
Ram L		.68	.68	.69	.68	.69	.76	.76	.76	.77	.76	.37	.39	.41	.43	.44	.73	.74	.74	.75	.75	.49	.50	.50	.51	.52	.51	.72	.72	.72	.72	.72

Carburetor duct pressure measurements, in pressure coefficient form $(h-p_o)/q_c$

Inlet

No	location	1	2	3	4	5	1	2	3	4	5	1	2	3	4	5	1	2	3	4	5	1	2	1	2	3	4	1	2	3	4	5
1	0	.78	.81	.80	-	-	.84	.86	.86	.82	.81	.37	.40	.41	.45	.46	.79	.80	.82	.80	.83	.46	.49	.49	.51	.49	.50	.84	.84	.85	.85	.85
2	.06	.91	.92	.93	.93	.92	.97	.98	.98	.99	.98	.37	.40	.42	.45	.47	.90	.92	.93	.94	.94	.42	.45	.45	.46	.48	.47	.97	.97	.98	.98	.99
3	.17	.95	.95	.96	.95	.96	.98	.99	.99	.99	.99	.39	.42	.45	.48	.49	.97	.98	.98	.98	.98	.42	.46	.46	.47	.49	.47	.98	.98	.99	1.00	1.00
4	.34	.96	.97	.97	.97	.97	.99	1.00	1.00	1.01	1.01	.48	.53	.55	.58	.61	.98	.99	.99	.99	1.00	.40	.50	.49	.51	.54	.52	.99	.99	1.00	1.01	1.02
5	.58	.96	.96	.96	-	-	1.00	1.01	1.01	1.01	1.01	.71	.73	.76	.78	.80	1.00	1.01	1.01	1.01	1.01	.62	.65	.64	.65	.69	.67	1.01	1.01	1.01	1.01	1.02
6	.84	.98	.97	.98	.98	.98	1.02	1.03	1.03	1.03	1.03	.90	.92	.92	.93	.93	1.02	1.02	1.03	1.03	1.03	.82	.84	.84	.85	.86	.85	1.02	1.03	1.03	1.03	1.03

Before carburetor elbow

No	location																															
7	.11	.66	.66	.67	.67	.68	.94	.95	.95	.96	.96	.61	.63	.65	.67	.68	.93	.94	.94	.94	.95	.59	.60	.61	.62	.62	.62	.85	.84	.82	.81	.79
8	.28	.77	.78	.78	.78	.79	.99	1.01	1.00	1.01	1.01	.68	.69	.71	.73	.73	.98	.99	.99	.99	.99	.60	.68	.69	.70	.72	.70	.97	.96	.95	.93	.92
9	.48	.95	.95	.96	.96	.96	1.01	1.01	1.01	1.02	1.02	.70	.73	.74	.76	.77	.99	1.01	1.01	1.01	1.01	.73	.74	.74	.75	.76	.75	1.01	1.01	1.01	1.01	1.02
10	.65	.96	.97	.97			1.02	1.02	1.02	1.03	1.03	.70	.73	.74	.75	.76	1.00	1.01	1.01	1.01	1.01	.73	.74	.75	.76	.77	.76	1.01	1.02	1.02	1.02	1.03
11	.83	.97	.97	.98	.98	.98	1.02	1.02	1.02	1.02	1.02	.72	.74	.75	.77	.78	1.00	1.01	1.01	1.02	1.02	.75	.76	.75	.76	.78	.77	1.02	1.02	1.02	1.02	1.02

After carburetor elbow

No	location																															
12	.12	.78	.78	.79	.79	.80	.89	.90	.90	.90	.90	.45	.48	.50	.52	.53	.88	.89	.89	.90	.89	.63	.64	.64	.66	.66		.83	.82	.82	.82	.82
13	.24	.80	.81	.81	.82	.82	.92	.92	.94	.94	.93	.51	.55	.55	.58	.58	.91	.91	.91	.92	.92	.64	.66	.67	.67	.68	.68	.85	.85	.85	.84	.84
14	.36	.83	.84	.85	.85	.86	.94	.96	.96	.96	.95	.56	.58	.61	.62	.63	.93	.94	.94	.94	.94	.66	.66	.68	.69	.69	.69	.88	.88	.88	.87	.86
15	.64	.93	.94	.94	.94	.94	.99	.99	.99	.99	.99	.64	.66	.68	.70	.71	.98	.98	.98	.98	.99	.71	.72	.73	.74	.75	.74	.98	.97	.98	.97	.97
16	.82	.94	.94	.95	.94	.94	.99	.99	.99	.99	.99	.66	.67	.70	.72	.73	.98	.98	.98	.98	.99	.72	.73	.75	.75	.77	.76	.98	.97	.98	.97	.97
17	.45	.89	.90	.90	.90	.91	.95	.96	.96	.96	.96	.53	.56	.57	.59	.60	.94	.95	.95	.95	.96	.69	.70	.71	.70	.72	.72	.94	.94	.95	.94	.94
18	.45	.90	.90	.91	.91	.91	.97	.98	.98	.98	.98	.55	.58	.59	.61	.62	.95	.95	.96	.96	.97	.69	.70	.71	.72	.73	.72	.95	.95	.95	.95	.95

Static pressure survey measurements, in pressure coefficient form $(p-p_o)/q_c$

Cowling lip over carburetor-air inlet

No	location	1	2	3	4	5	1	2	3	4	5	1	2	3	4	5	1	2	3	4	5	1	2	1	2	3	4	1	2	3	4	5
19	0	-.67	-.62	-.60	-.59	-.56	-.05	-.03	-.02	-.01	+.01	-.02	+.02	+.02	+.04	+.09						Greater than .40						-.08	-.07	-.06	-.04	-.02
20	.03	-2.00	-2.00	-1.92	-1.91	-1.90	-1.73	-1.69	-1.71	-1.65	-1.63	-1.19	-1.12	-1.11	-1.03	-1.04	+.18	+.20	-	-	-	-.56	-.46	-.49	-.46	-.38	-.42	-2.04	-1.98	-1.92	-1.90	-1.89
21	.19	-1.90	-1.93	-1.85	-1.84	-1.79	-1.65	-1.61	-1.61	-1.56	-1.54	-2.18	-2.10	-2.01	-1.92	-1.85	.18	+.15	.12	-.11	-.09	-.77	-.68	-.70	-.67	-.61	-.64	-1.72	-1.70	-1.65	-1.64	-1.60
22	.35	-1.80	-1.78	-1.75	-1.76	-1.74	-1.31	-1.29	-1.25	-1.19	-1.19	-1.54	-1.48	-1.43	-1.38	-1.32	-.30	-.27	-.25	-.24	-.20	-.77	-.68	-.71	-.67	-.63	-.67	-1.42	-1.37	-1.31	-1.26	-1.20
23	2.25	-.96	-.91	-.90	-.85	-.81	-.79	-.78	-.78	-.76	-.76	-.99	-.96	-.96	-.94	-.93	-.72	-.71	-.72	-.69	-.70	-.80	-.80	-.78	-.79	-.77	-.76	-.72	-.72	-.70	-.71	-.68
24	5.50	-.70	-.72	-.70	-.70	-.70	-.68	-.67	-.68	-.66	-.66	-.89	-.88	-.87	-.86	-.84	-.94	-.93	-.92	-.89	-.89	-1.15	-1.11	-1.13	-1.10	-1.07	-1.09	-.83	-.83	-.81	-.80	-.79
25	14.50	-.40	-.40	-.39	-.39	-.39	-.41	-.40	-.40	-.39	-.39	-.45	-.45	-.44	-.44	-.43	-.44	-.44	-.44	-.43	-.36	-.46	-.45	-.45	-.46	-.43	-.44	-.42	-.42	-.41	-.40	-.39

Lower inlet lip

No	location																															
26	0	.49	.53	.53	.54	.56	.94	.95	.93	.89	.87	.07	.10	.11	.12	.14	.82	.85	.86	.85	.88	.26	.30	.30	.32	.31	.32	.92	.93	.93	.92	-
27	.1	.50	.51	.50	.52	.54	.88	.88	.88	.89	.87	.05	.06	.07	.07	.07	.44	.47	.49	.49	.53	.24	.25	.27	.30	.27	.28	.84	.87	.87	.87	.88
28	.3	.56	.59	.57	-	-	.82	.81	.82	.80	.82	.19	.20	.21	.22	.23	.62	.64	.66	.66	.68	.36	.36	.37	.39	.38	.37	.79	.80	.80	.80	.82
29	2.0	.74	.76	.75	-	-	.83	.84	.84	.82	.81	.24	.27	.28	.32	.33	.72	.72	.74	.73	.75	.37	.38	.39	.40	.40	.38	.83	.83	.84	.84	.84

Abbreviation definitions and explanations

Configuration
- inlet — carburetor-air inlet
- elb — carburetor duct elbow
- Sp — spinners
- Dg — Douglas
- def pl — deflector plates

Airplane conditions
- Q_c — airplane impact pressure
- Q_o — free-stream dynamic pressure
- P_o — altitude pressure
- L — left engine

Carburetor duct pressure measurements
- h — measured total pressure
- No — pressure tube number identified on figure 2
- location — approximate tube height above engine side surface of duct in terms of duct height at survey. All tubes except 17 & 18 are in duct & Tubes 17 & 18 close to duct sides after elbow

Static pressure survey measurements
- p — static pressure at orifice
- No — static orifice number identified on figure 2
- location — approximate distance aft of respective lip in inches

NATIONAL ADVISORY
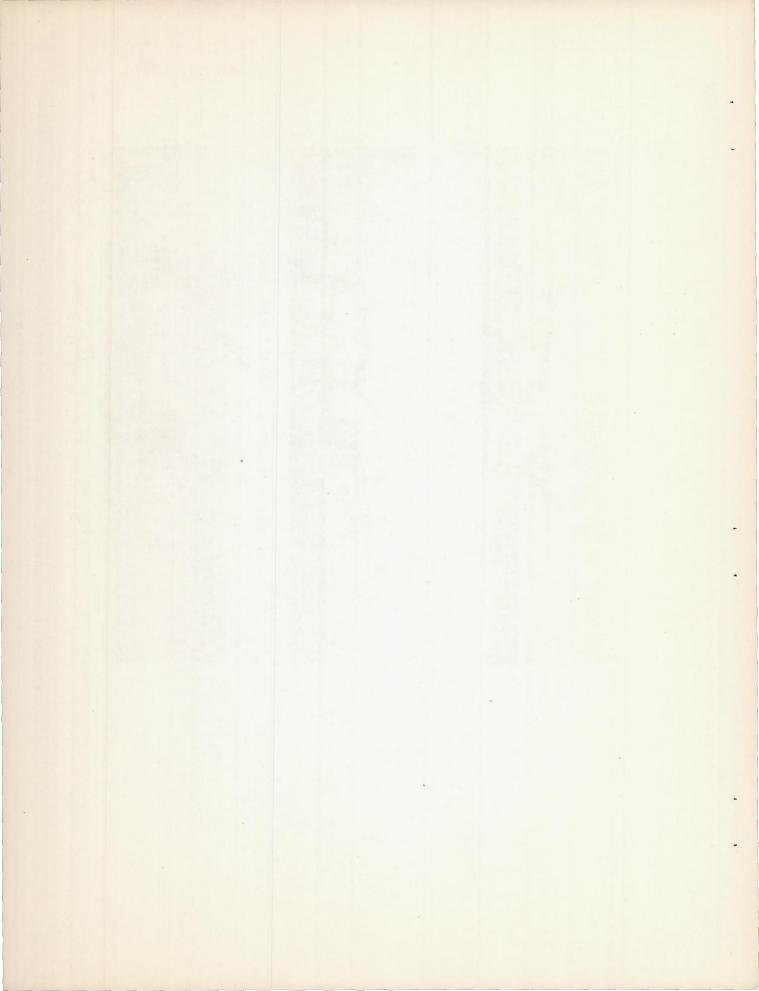COMMITTEE FOR AERONAUTICS
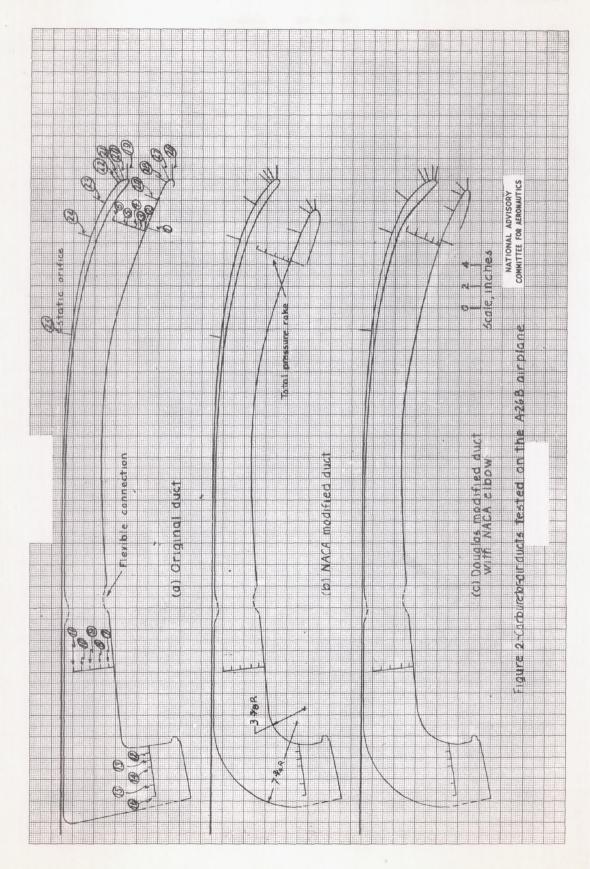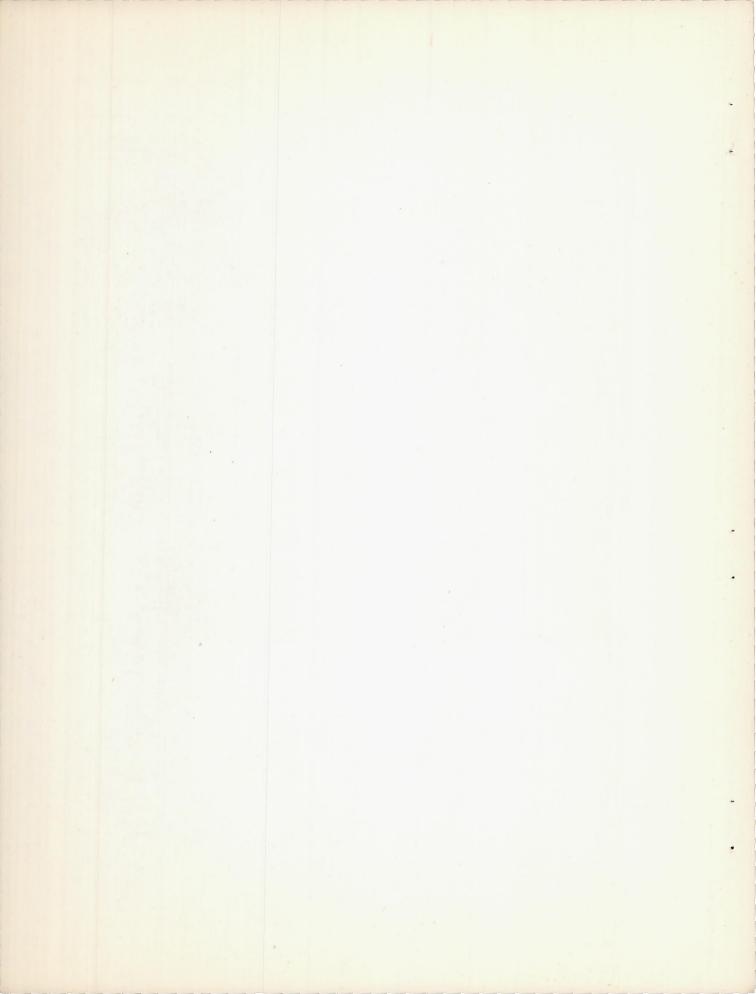
(a) Front view.

(b) Three-quarter right front view.

(c) Left side view.

Figure 1.- General views of the production A-26B airplane after instrumentation.

(a) Original duct

(b) NACA modified duct

(c) Douglas modified duct with NACA elbow

Static orifice

Flexible connection

Total pressure rake

0   2   4

Scale, inches

NATIONAL ADVISORY
COMMITTEE FOR AERONAUTICS
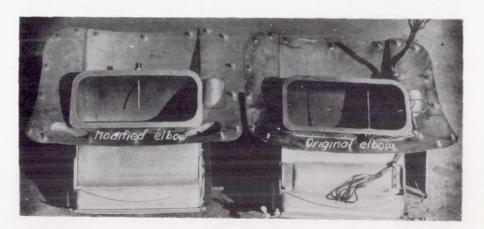
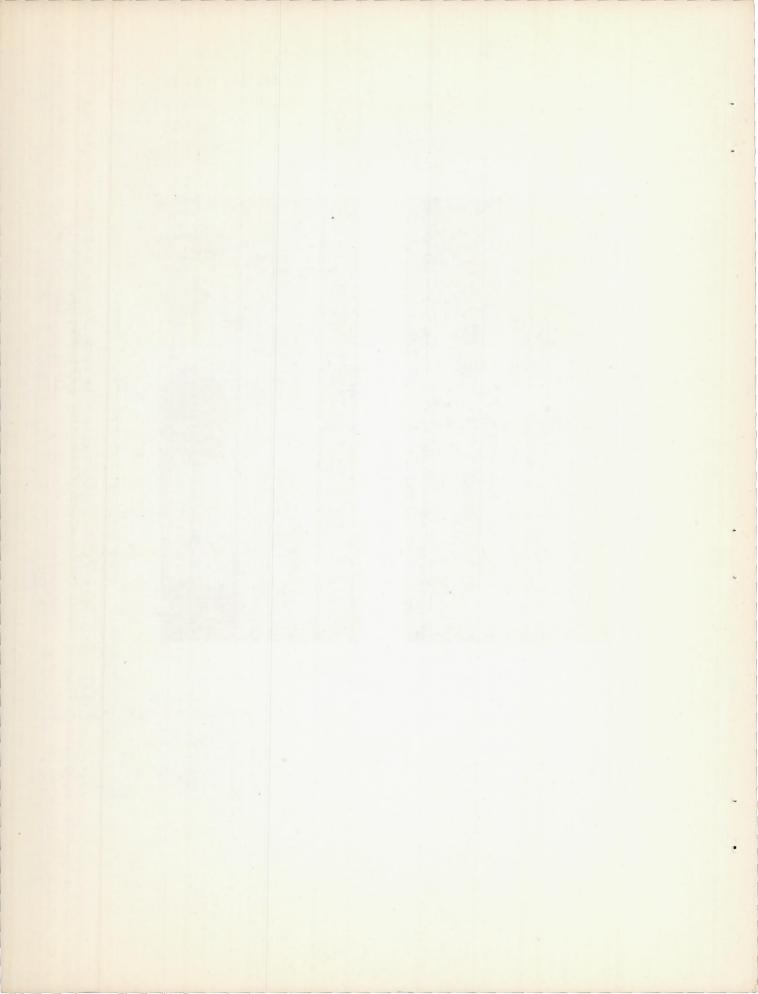Figure 2.- Carburetor air ducts tested on the A-26B airplane.

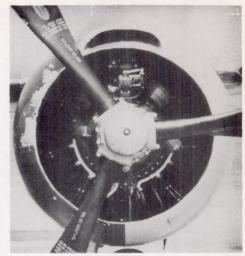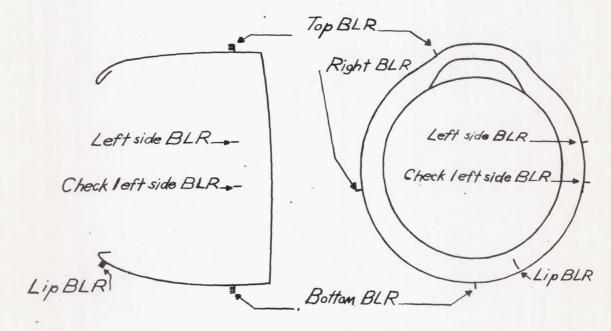(a) Engine side or inner radius of bend.

(b) Outer radius of bend.

Figure 3.- Carburetor duct elbows tested on the A-26B airplane as
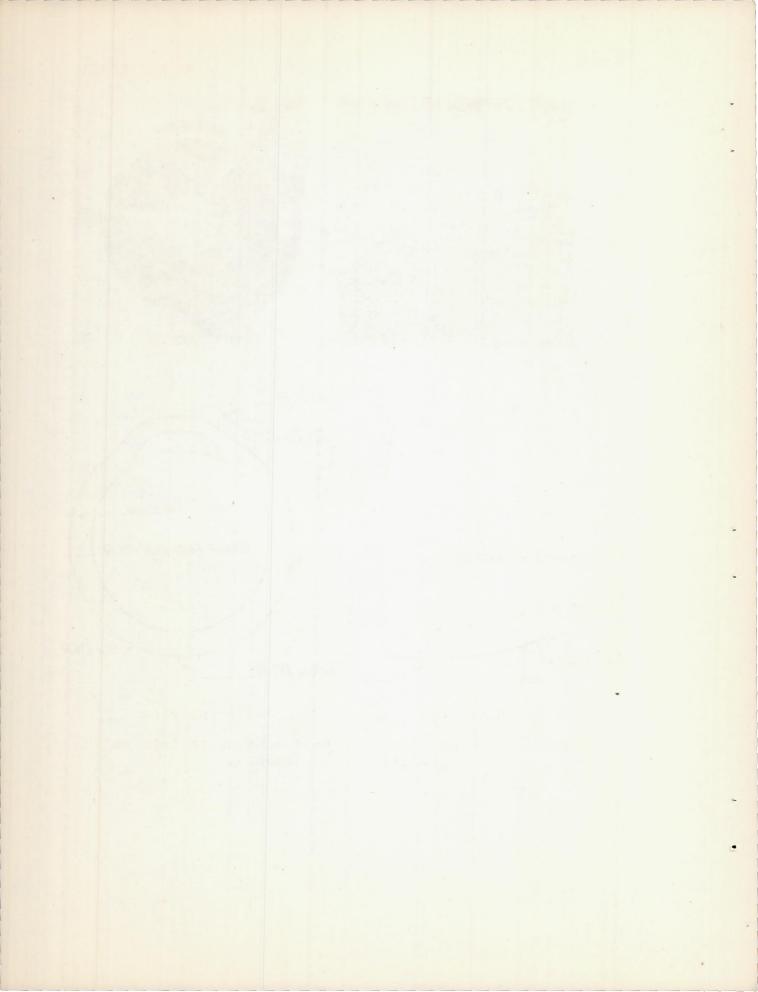seen from the carburetor.

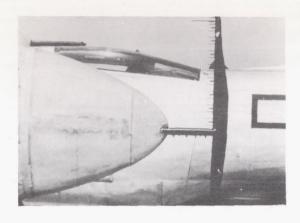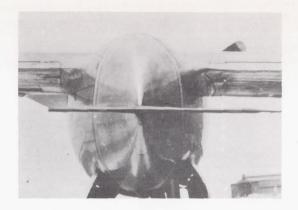(a) Side view.   (b) Front view.

Figure 4.- Boundary layer rake locations on left engine cowling A-26B airplane.
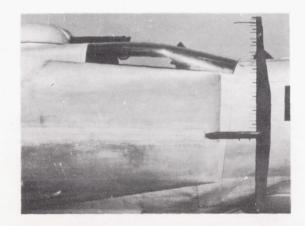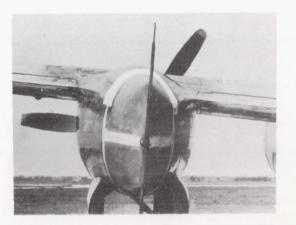
(a) Side, rake in upright starting position.   (b) Rear view with rake revolving.

Original Afterbody.
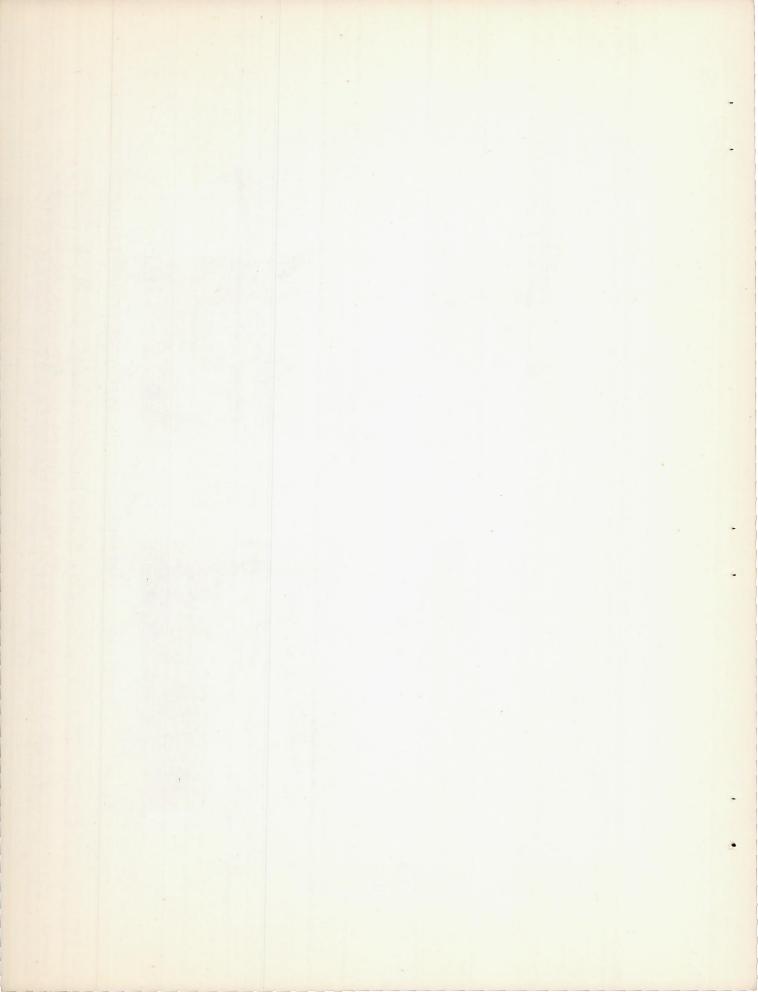
c) Side view modified afterbody.   (d) Rear view modified afterbody.

Modified nacelle afterbody.
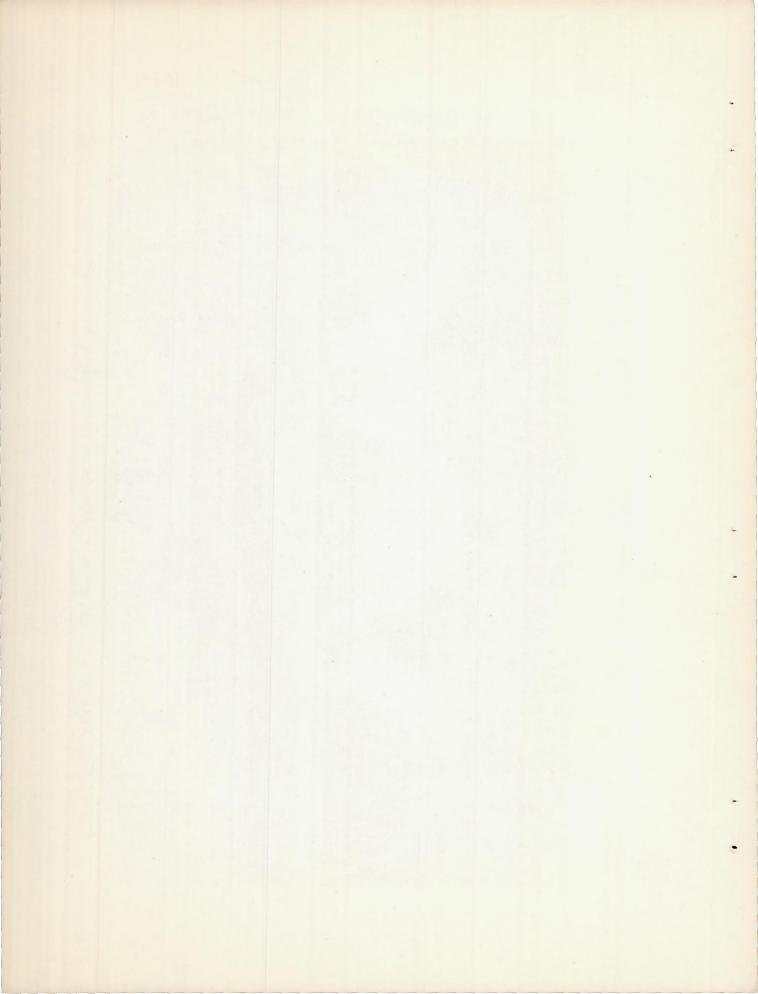
Figure 5.- Left engine nacelle afterbodies of the A-26B airplane.

(a) Original.   (b) NACA modified.   (c) Douglas modified.

Figure 6.- Carburetor air inlets tested on the A-26B airplane.
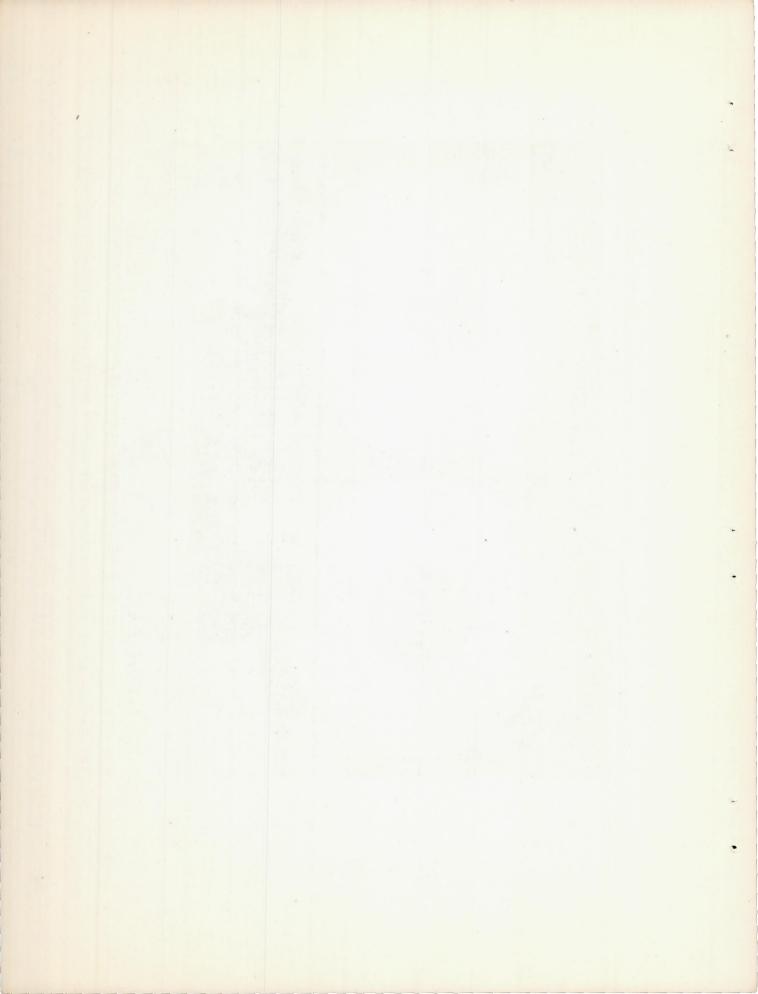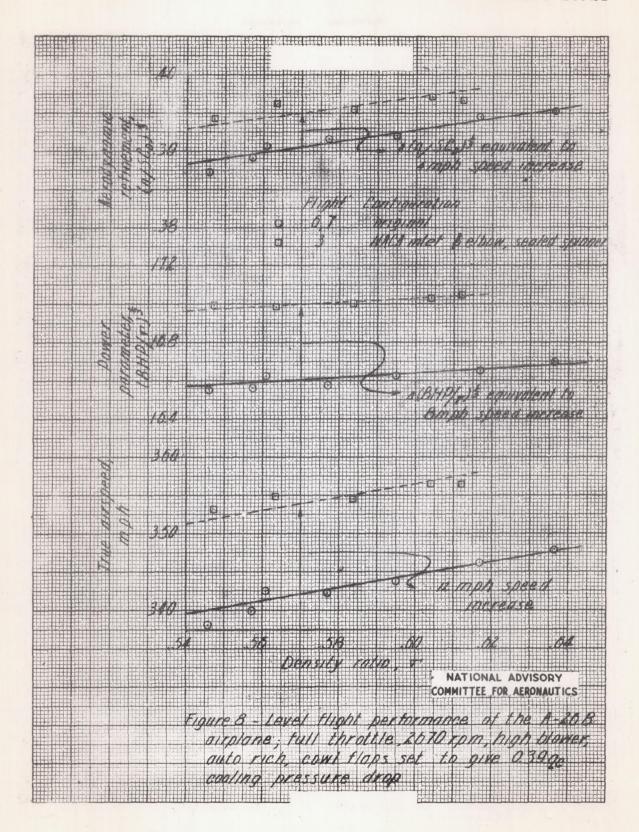
(a) Original.   (b) Sealed.
            (c) The seal removed.

Figure 7.- Spinner rear bulkhead of A-26B airplane as seen from engine.

Figure 8 - Level flight performance of the A-26B airplane; full throttle, 2670 rpm, high blower, auto rich, cowl flaps set to give 0.39 q_c cooling pressure drop
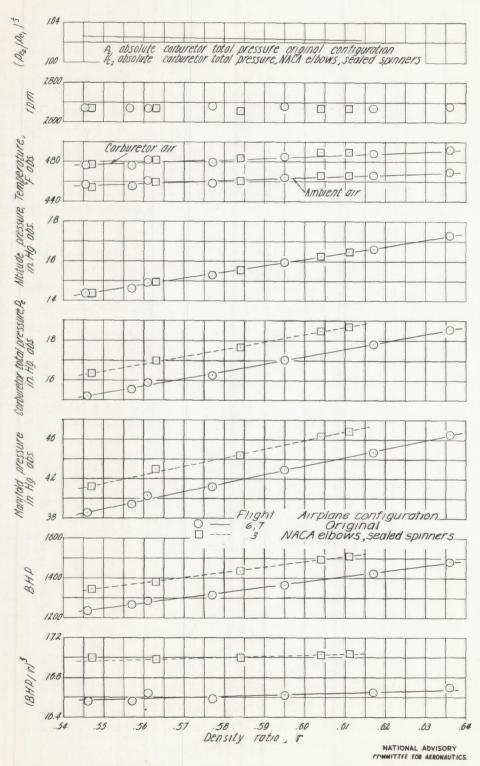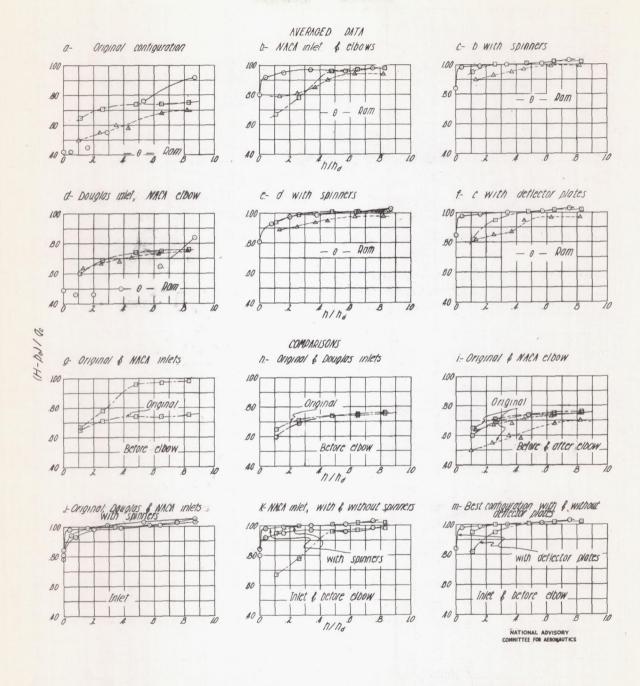
Figure 9.— Factors affecting the power parameter as functions of density ratio, averaged for two engines.

L-740

AVERAGED DATA

a- Original configuration

b- NACA inlet & elbows

c- b with spinners

— 0 — Ram

h/h_d

d- Douglas inlet, NACA elbow

e- d with spinners

f- c with deflector plates

— 0 — Ram

h/h_d

— 0 — Ram

$(H-p_o)/Q_o$

COMPARISONS

g- Original & NACA inlets

Original

Before elbow

h- Original & Douglas inlets

Original

Before elbow

h/h_d

i- Original & NACA elbow

Original

Before & after elbow

j- Original, Douglas & NACA inlets with spinners

Inlet

k- NACA inlet, with & without spinners

with spinners

Inlet & before elbow

h/h_d

m- Best configuration with & without deflector plates

with deflector plates

Inlet & before elbow

Note: h height of tube in survey plane above engine side surface of duct
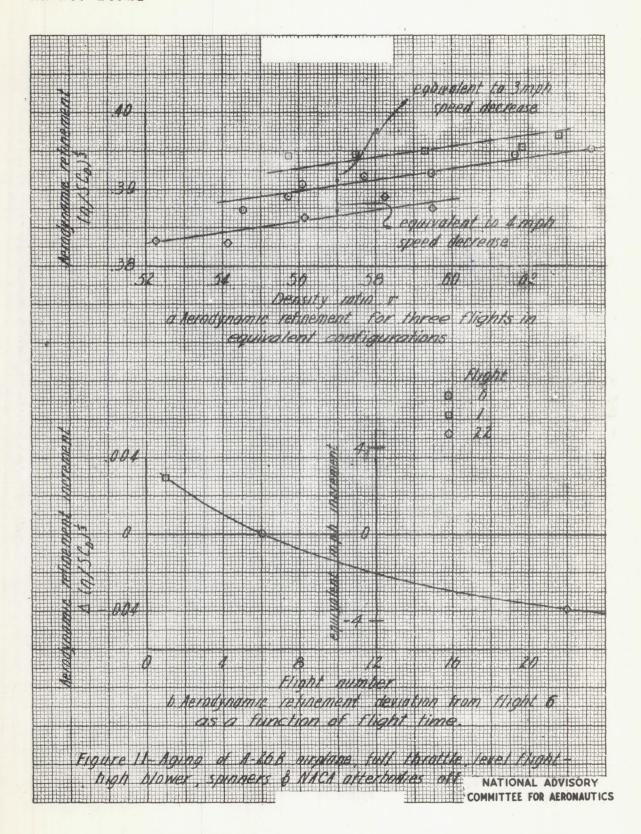h_d height of duct at survey plane
H local total pressure
p free-stream static pressure
Q_o airplane impact pressure
H-p_o local total pressure above free-stream static

○ —— survey plane at inlet
□ —·— survey plane before elbow
△ ----- survey plane after elbow

Figure 10.- Total pressure distributions in the various portions of the original & modified charge air ducts

a aerodynamic refinement for three flights in equivalent configurations

b Aerodynamic refinement deviation from flight 6 as a function of flight time.

Figure 14 Aging of A-26B airplane, full throttle, level flight - high blower, spinners & NACA afterbodies off

Aerodynamic refinement parameter $(n/SC_D)^{\frac{1}{3}}$

a. Sealed spinners

equivalent to 4 mph speed increase

Flight	Configuration
6,7	original
3	sealed spinners

b. Sealed spinners, modified nacelle afterbodies

equivalent to 4 mph speed increase

Flight	Configuration
6,7	original
16,17	sealed spinners, modified nacelle afterbodies

c. Modified nacelle afterbodies, spinners off

equivalent to 2 mph speed increase

Flight	Configuration
6,7	original
18,19	modified nacelle afterbodies

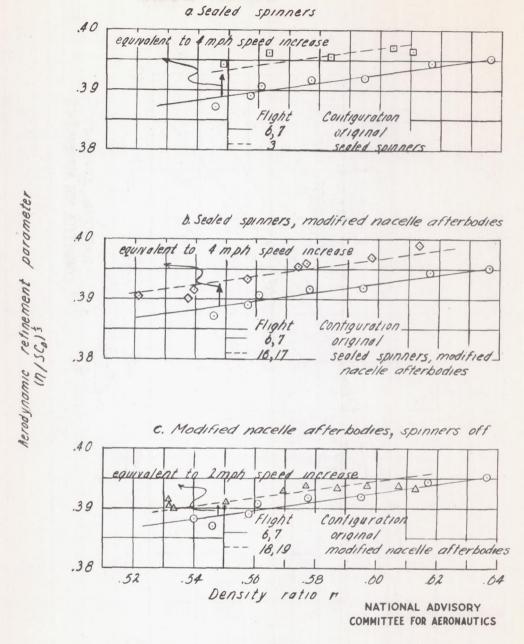Density ratio r

NATIONAL ADVISORY
COMMITTEE FOR AERONAUTICS

Figure 12.- Effect of sealed spinners and of modified afterbodies on aerodynamic refinement parameter of A-26B airplane; full throttle, high blower level flight
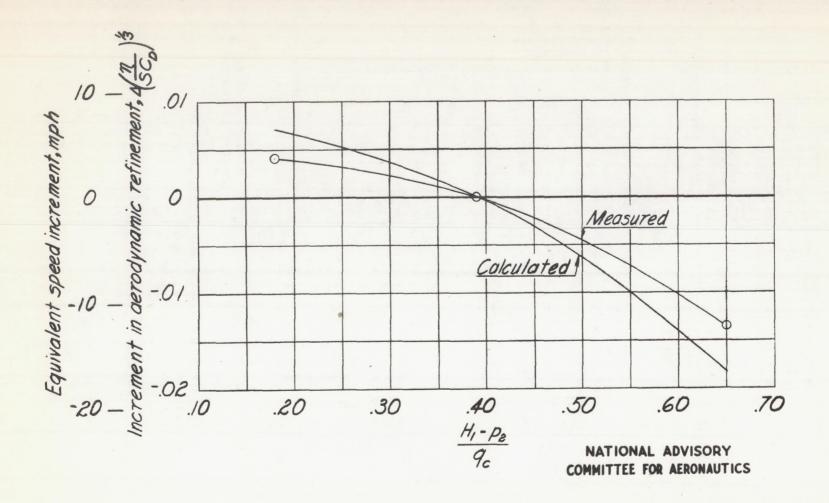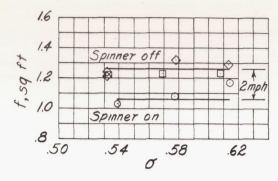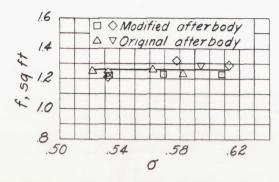
Figure 13.- Comparison of the calculated and measured variation of the aerodynamic refinement parameter with engine cooling air pressure drop coefficient. Spinner off.
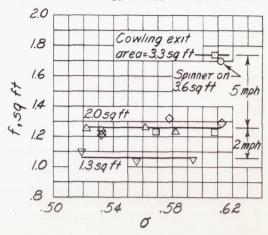
(a) Effect of removing spinner.

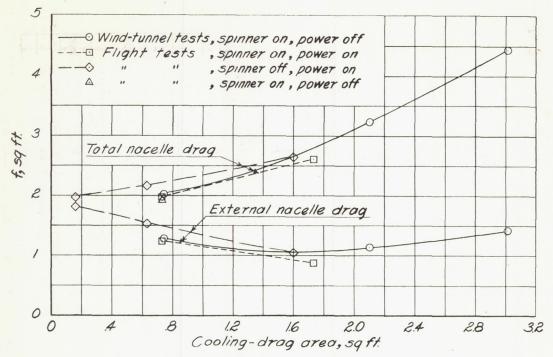| Symbol	Flight no.
○	17
□	18
◇	19
△	22
▽	24

NATIONAL ADVISORY
COMMITTEE FOR AERONAUTICS
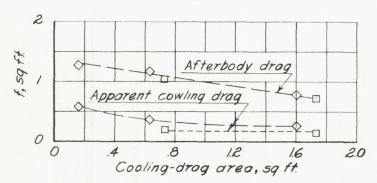
(b) Effect of modified nacelle afterbody,
spinner off.

(c) Effect of cowling exit area. Spinner
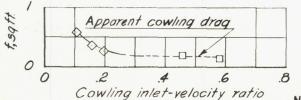off except as indicated.

Figure 14.- Drag of left engine nacelle of A-26B airplane as measured by
survey rake. Speed increments are for one nacelle.

(a) Variation of total nacelle drag and external nacelle drag with cooling drag.

(b) Variation of afterbody drag and apparent cowling drag with cooling drag.

NATIONAL ADVISORY
COMMITTEE FOR AERONAUTICS

(c) Variation of apparent cowling drag with cowling inlet-velocity ratio.

Figure 15.- Comparison of nacelle drag components from flight and wind-tunnel results.

(a) Spinner off,
Cowling exit area 1.3 sq ft

(b) Spinner off,
Cowling exit area 2.0 sq ft

(c) Spinner off,
Cowling exit area 3.3 sq ft

(d) Spinner on,
Cowling exit area 2.0 sq ft

(e) Spinner on,
Cowling exit area 3.6 sq ft

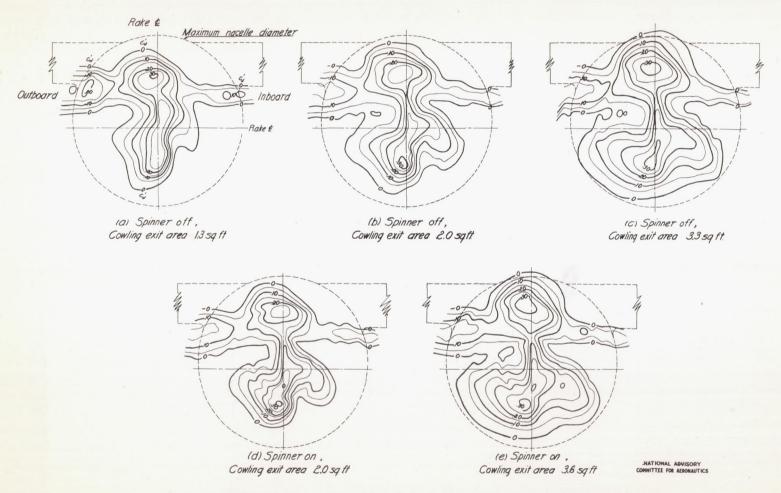NATIONAL ADVISORY
COMMITTEE FOR AERONAUTICS

Figure 16.- Distribution of point drag coefficient in wake of left engine nacelle of A-26B airplane.

CONFIDENTIAL